

Circularly Polarized Rectangular Ring-Slot Antenna with Chamfered Corners for Off-Body Communication at 5.8 GHz ISM Band

Petr VASINA, Jaroslav LACIK

Dept. of Radio Electronics, Brno University of Technology, Technicka 12, 616 00 Brno, Czech Republic

xvasin05@stud.feec.vutbr.cz, lacik@feec.vutbr.cz

Submitted October 4, 2016 / Accepted January 28, 2017

Abstract. This paper deals with a substrate integrated waveguide (SIW) circularly polarized rectangular ring-slot antenna with chamfered corners designed for 5.8 GHz ISM frequency band for off-body communication. The antenna consists of a substrate integrated waveguide, which operates in the fundamental mode TE_{10} , and the rectangular ring-slot radiator with chamfered corners etched in the top wall of the SIW. It radiates a right-handed circularly polarized (RHCP) wave in the boresight direction. Experimental results prove that the proposed antenna located in free space achieves the impedance bandwidth of 2.41 % (for the reflection coefficient less than -10 dB) and the RHCP gain of 6.57 dBi, and the impedance bandwidth of 2.6 % and the RHCP gain of 6.98 dBi for its location on the phantom. The axial ratio (AR) bandwidth (for the AR less than 3 dB) is 0.9 % for both configurations.

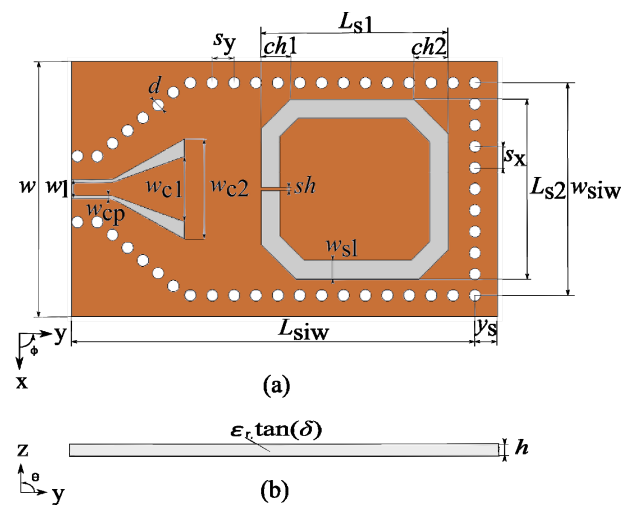


Fig. 1. Proposed antenna configuration: (a) top view and (b) side view.

Keywords

Substrate integrated waveguide, off-body communication, rectangular ring slot antenna, circular polarization

1. Introduction

The electronic devices miniaturization tends to development of wearable equipments. Thus, a body-centric communication (BCC) system for occupation or entertainment has been investigated. In general, antennas in such systems should be insensitive to surrounding environment, wearable, of light weight and low cost, easily fabricated and almost maintenance-free.

The substrate integrated waveguide (SIW) technology [1] seems to be a promising technology for BCC. The advantages, such as simple fabrication, small size, low profile, low loss, and easy integration with planar structures, are supported by the fact that this technology allows a reduction of radiation towards a body. Further, SIW based antennas have usually small sensitivity to the surrounding environment. Possible SIW antenna candidates

for off-body communication were presented in [2–6]. In [2], the two-pole filtering antenna based on a SIW resonator for BCC is presented. The simulated reflection coefficient of the antenna was less than -20 dB in the whole 5.8 GHz ISM band and the simulated realized gain was 9.34 dBi. Unfortunately, the antenna has two-layer configuration. To reduce the dimensions and complexity of the antenna, single layer antennas based on a quarter-mode SIW topology were proposed [3], [4]. The antennas reached stable on-body performance. The maximal reached gain of the antenna [4] was 5.16 dBi with the measured fractional bandwidth of 2.0 % for 5.8 GHz ISM frequency band. In [5], the authors published the miniaturized folded cavity backed crossed-slot antenna. They stated a 72.8 % size reduction in comparison with a conventional cavity backed antenna. A further step was the redesign of the antenna for the textile substrate. Although the antenna concepts [3–5] have good impedance and radiation properties, they have the disadvantage of using a coax-to-SIW transition from their bottom side which limits their exploitation for BCC. In [6], a concept of the Koch slot loop antenna with tuning stub equipped by a coax-to-SIW transition in the antenna plane was proposed. The Koch snowflake was created from the third interaction of the Koch

fractal. The antenna operated in the whole 5.8 GHz ISM frequency band and reached the gain of 5.97 dBi on a duke phantom.

A common feature of antennas for off-body communication is that they radiate usually linearly polarized wave. However, due to the surrounding environment, the depolarization of the electromagnetic wave can occur [7]. Fortunately, the circular polarization can solve problems of polarization interference and mismatch from the surrounding environment [8]. In addition, exploitation of circularly polarized antennas in the area of BCC is beneficial since the position of the antenna can be changed by the movement of the human body.

In this paper, a concept of a SIW circularly polarized rectangular ring-slot antenna with chamfered corners is proposed. It is based on a linearly polarized SIW rectangular ring-slot radiator [9]. The proposed antenna is low profile, it has a single-layer configuration and good radiation performance.

2. Configuration of the Proposed Antenna

The configuration of the proposed antennas is depicted in Fig. 1. On both sides, the dielectric substrate of the length $L_{siw} + y_s$, the width w , and the height h with relative permittivity ϵ_r is covered by conductive sheets. The SIW is created by two rows of vias of the width w_{siw} . The diameter of the vias is d and their spacing is s . The SIW operates in the fundamental mode TE_{10} , and its one end is shorted. The rectangular ring slot of the lengths $L_{s1} \times L_{s2}$ and the width w_{s1} with chamfered corners is etched in the top conductive layer in the proximity of the shorted end of the SIW. The antenna is equipped by a ground coplanar waveguide (GCPW)-to-SIW transition [10].

The antenna radiates a right-hand circularly polarized (RHCP) wave in the boresight direction. The left-hand circularly polarized (LHCP) wave can be obtained by mirroring the rectangular slot with respect to the longitudinal axis of the antenna.

3. Design of Antenna and Simulated Results

The antenna in Fig. 1 without the GCPW-to-SIW transition was designed by the following steps:

- Design of the SIW using the relations presented in [1]: The SIW operates in the fundamental mode TE_{10} . The operating frequency of the antenna is approximately 1.5 times higher than the cut-off frequency of the fundamental mode. In order to decrease the computation cost of the design procedure, during the design, the SIW can be substituted by the equivalent rectangular waveguide.

- Determination of the radiator position: The center of the radiator should be placed in the distance of approximately $\lambda_g/4$, where λ_g is the wavelength in the SIW at the design frequency, from the shorted end of the SIW in the y -direction.
- Preliminary determination of the radiator dimensions: The perimeter of the rectangular ring-slot (dimensions L_{s1} and L_{s2}) should be less than λ_g . To obtain acceptable impedance matching the short of width sh must be placed in the bottom part of the slot. The circular polarization should be achieved by setting an appropriate ratio of the size of chamfered corners.
- The optimization procedure with combination of a full wave solver has to be applied in order to tune the antenna for the desired operating frequency band.

After the design, the antenna was equipped by GCPW-to-SIW transition whose dimensions were determined with the help of the design relations presented in [10].

The proposed antenna was designed for the ISM frequency band 5.8 GHz with help of CST Microwave studio on the substrate Arlon CuClad217 with relative permittivity $\epsilon_r = 2.2$ and thickness $h = 0.7874$ mm. The width of SIW ($w_{siw} = 25.79$ mm) is designed for operating frequency 5.8 GHz in the fundamental mode. The cutoff frequency of the fundamental TE_{10} mode is 3.8 GHz. The resultant dimensions of the proposed antenna are summarized in Tab. 1.

The distribution of the electric intensity at frequency of 5.8 GHz is depicted in Fig. 2. Owing to chamfered corners, two nearby modes are excited. The antenna radiates circularly polarized wave in the boresight direction (Fig. 5, 6).

The antenna performance in free space and then on a muscle-equivalent phantom (relative permittivity $\epsilon_r = 48.5$ and electric conductivity $\sigma = 4.96$ S/m at 5.8 GHz [11]) was simulated to investigate the effect of the phantom on the antenna behavior. The distance between the antenna and the phantom was 4 mm. The shape of the phantom was a right square prism of overall dimensions of 200 mm \times 200 mm \times 20 mm.

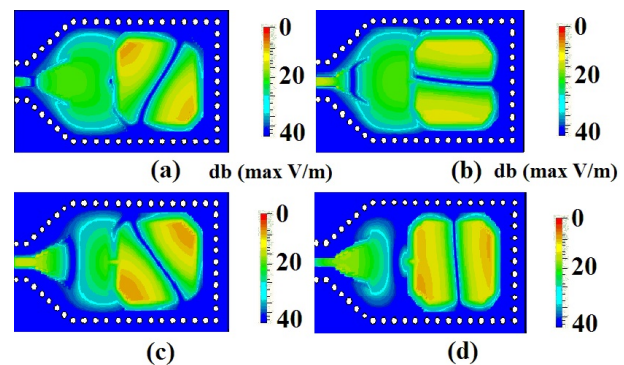


Fig. 2. Distribution of electric field at frequency 5.8 GHz: (a) phase = 0°, (b) phase = 45°, (c) phase = 90°, and (d) phase = 135°.

Parameters	Dimensions [mm]	Parameters	Dimensions [mm]
ch_1	2.23	L_{siw}	49.2
ch_2	2.89	sh	0.27
d	1.40	s_x	5.58
h	0.7874	s_y	2.66
L_{s1}	18.14	w	31.0
L_{s2}	17.13	wc_1	7.94
w_{siw}	25.79	wc_2	12.1
w_{s1}	2.40	wcp	0.37
y_s	2.52	w_1	1.64

Tab. 1. Parameters of the proposed antenna.

The simulated results are depicted in Fig. 3–6. The results show that the phantom has a very small effect on the reflection coefficient and the axial ratio of the antenna (Fig. 3 and 4). For both configurations, the reflection coefficient of the antenna is sufficiently low (less than -10 dB) in the whole 5.8 GHz ISM frequency band (from 5.725 to 5.875 GHz). The axial ratio achieves the bandwidth (less than 3 dB) of 48 MHz in free space and 42 MHz on the phantom. The proximity of the phantom slightly moves curves to the lower frequencies.

The simulated normalized radiation patterns in two orthogonal planes are depicted in Fig. 5 and 6. The maximum radiation of the antenna is in the perpendicular direction to the antenna plane. The radiation pattern of the antenna placed on the phantom has a little wider main lobe. The simulated RHCP gain of the antenna is 7.09 dBi in free space and 6.89 dBi on the phantom.

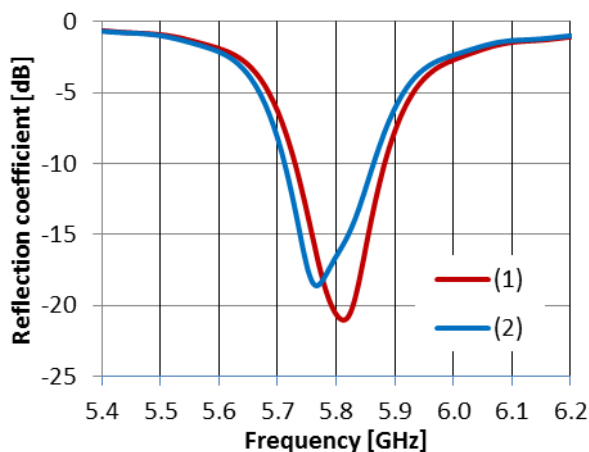


Fig. 3. Simulated reflection coefficient of the proposed antenna: (1) in free space and (2) on the phantom.

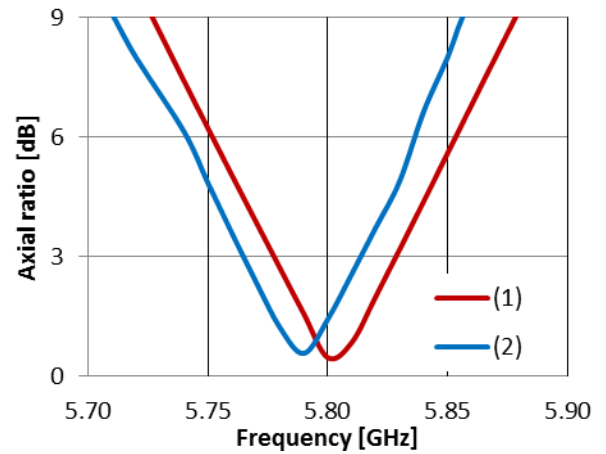


Fig. 4. Simulated axial ratio of the proposed antenna: (1) in free space and (2) on phantom.

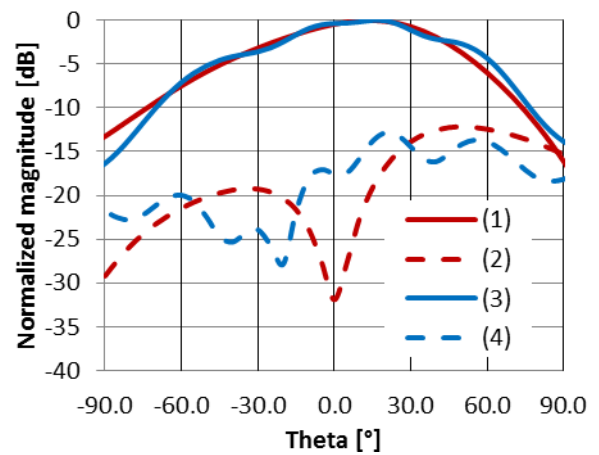


Fig. 5. Simulated normalized radiation pattern of the proposed antenna in y - z plane: (1) in free space RHCP, (2) in free space LHCP, (3) on phantom RHCP, and (4) on phantom LHCP.

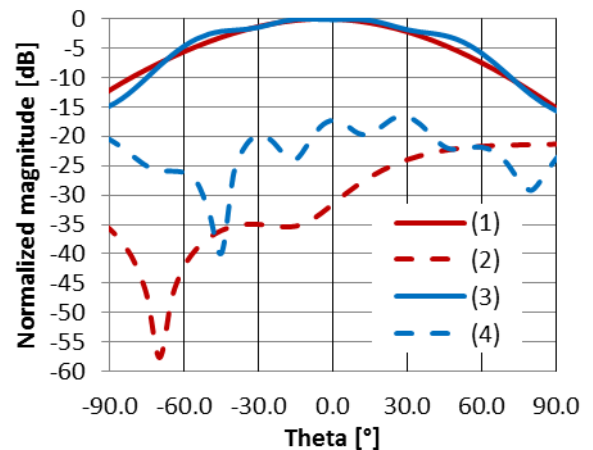


Fig. 6. Simulated normalized radiation pattern of the proposed antenna in x - z plane: (1) in free space RHCP, (2) in free space LHCP, (3) on phantom RHCP, and (4) on phantom LHCP.

4. Parametric Study

To understand the antenna behavior, a parametric study has been performed. The effect of varying the slot length L_{s1} and the slot length L_{s2} on the reflection coefficient and the axial ratio is depicted in Fig. 7(a, b). We observe L_{s1} parameter influences the operating frequency. Increasing the value of the slot length leads to the decrease of the operating frequency. The effect of this parameter on the axial ratio is very small. The slot length L_{s2} influences mainly the impedance matching of the antenna and the axial ratio. Increasing the slot length L_{s2} leads to decreasing the minimum of the axial ratio on the frequency axis.

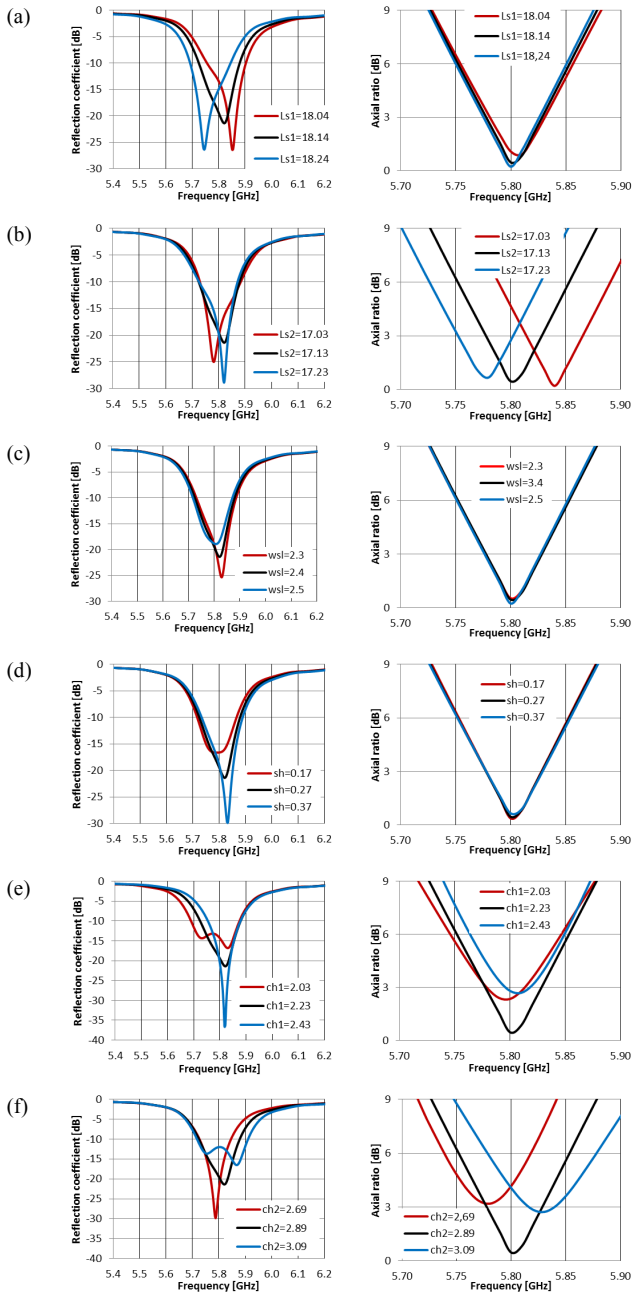


Fig. 7. Parametric analysis and effect on reflection coefficients: (a) slot length L_{s1} , (b) slot length L_{s2} , (c) width of slots, (d) width of short, and (e, f) dimension of chamfered corners.

Figure 7(c, d) shows the effect of the slot width wsl and the width of the short sh . Both parameters influence mainly the impedance matching of the antenna. Their influence on the axial ratio is negligible.

The last two parameters tested in this parametric study are dimensions of chamfered corners $ch1$, $ch2$ (Fig. 7(e, f)). Obviously, these parameters have very significant effect on the exciting of two nearby modes, and consequently on the axial ratio and the impedance matching of the antenna.

5. Experimental Results

The proposed antenna was fabricated by a low-cost etching PCB process (Fig. 8). To carry out a conventional coaxial measurement, the antenna was equipped by an SMA connector. The measurement was done in free space and on a muscle-equivalent phantom [12] whose shape was a right square prism of overall dimensions $200\text{ mm} \times 200\text{ mm} \times 20\text{ mm}$. The distance between the antenna and the phantom was 4 mm.

The measured reflection coefficient of the antenna is depicted in Fig. 9. We can see that the antenna is very well matched in the whole 5.8 GHz ISM band. The impedance bandwidth of the antenna for the reflection coefficient less than -10 dB is 2.4 % and 2.6 % for the antenna placed in free space and on the phantom, respectively. The difference between the results when the antenna is placed in free space and on the phantom is very small and it can be neglected.

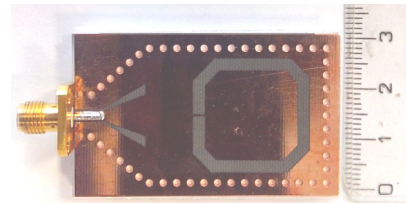


Fig. 8. The manufactured sample of the proposed antenna.

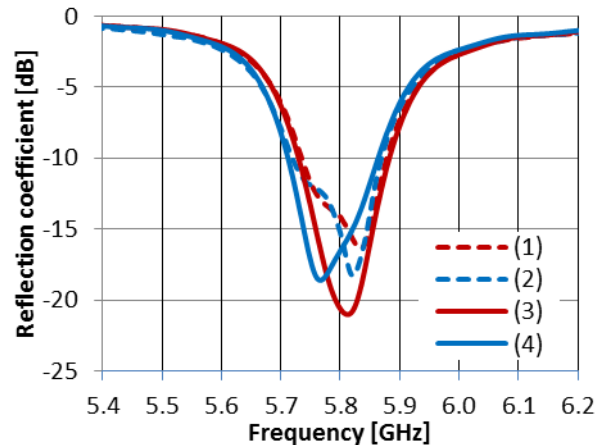


Fig. 9. Measured (dashed line) and simulated (solid line) reflection coefficient of the proposed antenna: (1, 3) in free space, and (2, 4) on phantom.

In Fig. 10, the axial ratio in the boresight direction is depicted. The measured axial ratio bandwidth is 0.9 % for its value lower than 3 dB for both configurations (in free space and on the phantom). Again, due to the phantom, the minimum axial ratio is shifted to lower frequencies as for the simulated data (Fig. 4). The slight difference between the simulated and measured results is caused due to fabrication tolerance, and probably due to a slightly different value of the relative permittivity of the substrate in comparison to that used for the design.

The antenna radiation pattern was measured in an anechoic chamber for the angle θ from -90° to 90° . The results for both orthogonal planes are depicted in Fig. 11 and 12. We observe that the phantom has a small effect on the copolar component (RHCP) of the radiated wave. The measured RHCP gain of the antenna placed in free space and on the phantom is 6.57 dBi and 6.98 dBi, respectively.

The measured gain of the antenna at the center frequency in free space and on the phantom is 6.57 dBi and 6.98 dBi, respectively. The measured radiation efficiency

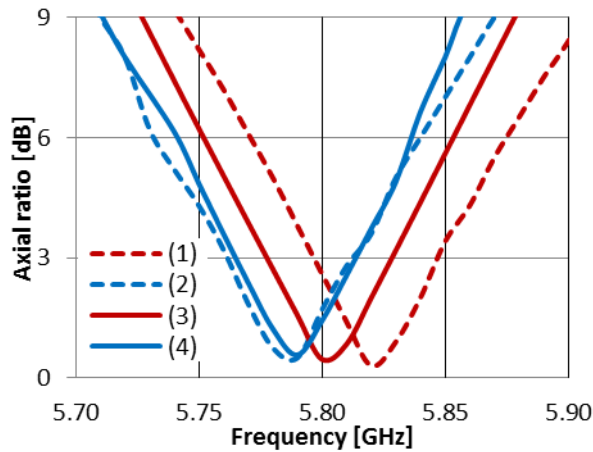


Fig. 10. Measured (dashed line) and simulated (solid line) axial ratio of the proposed antenna: (1, 3) in free space, and (2, 4) on phantom.

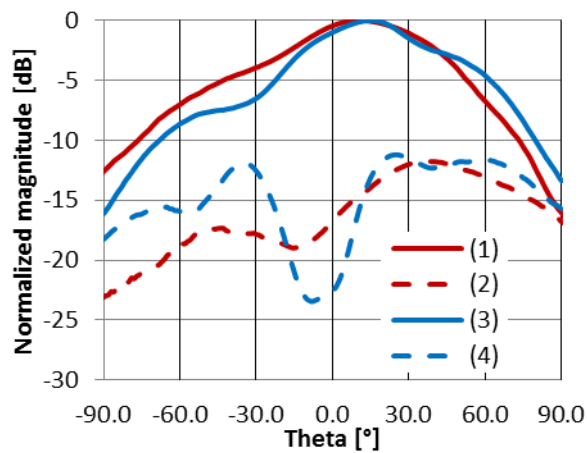


Fig. 11. Measured normalized radiation pattern of the proposed antenna in y - z plane: (1) in free space RHCP, (2) in free space LHCP, (3) on phantom RHCP, and (4) on phantom LHC.

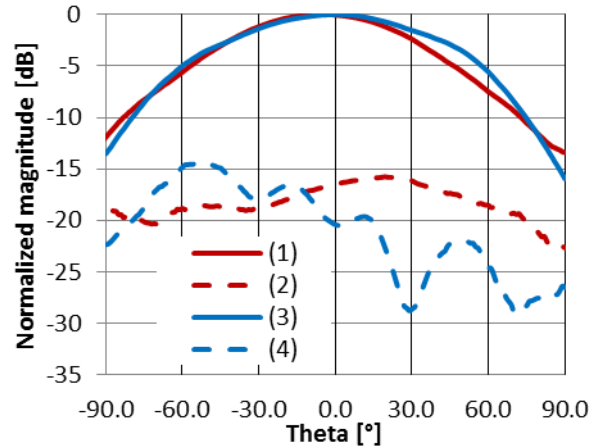


Fig. 12. Measured normalized radiation pattern of the proposed antenna in x - z plane: (1) in free space RHCP, (2) in free space LHCP, (3) on phantom RHCP, and (4) on phantom LHC.

of the antenna (defined as the measured gain over the simulated directivity) in free space and on the phantom is 86.8 % and 87 %, respectively.

6. Conclusion

Circularly polarized rectangular ring-slot antenna with chamfered corners has been proposed. It operates in 5.8 GHz ISM frequency band, and radiates a right-hand circularly polarized (RHCP) in the boresight direction. Since the antenna is low profile, has good radiation performance, and radiates circularly polarized wave, it seems to be a promising solution for off-body communications.

Acknowledgments

The presented research was supported by the Czech Science Foundation (GACR) project no. P102/12/1274 and by the Czech Ministry of Education in frame of the National Sustainability Program under grant LO1401. The research is the part of the COST Action IC1301 which is financially supported by the grant of the Czech Ministry of Education no. LD14057. For research, infrastructure of the SIX Center was used.

References

- [1] BOZZI, M., GEORGIADIS, A., WU, K. Review of substrate integrated waveguide (SIW) circuits and antennas. *IET Microwaves, Antennas & Propagation*, 2011, vol. 5, no. 8, p. 909 to 920. DOI: 10.1049/iet-map.2010.0463
- [2] WOLANSKY, D., HEBELKA, V., RAIDA, Z. Two-pole filtering antenna for body centric communications. In *Proceedings of the Loughborough Antennas and Propagation Conference (LAPC)*. The Loughborough (United Kingdom), 2013, p. 221–224. DOI: 10.1109/LAPC.2013.6711887

- [3] AGNEESSENS, S., LEMEY, S., VERVUST, T., ROGIER, H. Wearable, small, and robust: The circular quarter-mode textile antenna. *IEEE Antennas and Wireless Propagation Letters*, 2015, vol. 14, p. 1482–1485. DOI: 10.1109/LAWP.2015.2389630
- [4] ZHU, X. Q., GUO, Y. X., WU, W. A compact dual-band antenna for wireless body-area network applications. *IEEE Antennas and Wireless Propagation Letters*, 2016, vol. 15, p. 98–101. DOI: 10.1109/LAWP.2015.2431822
- [5] MORO, R., AGNEESSENS, S., ROGIER, H., et al. Textile microwave components in substrate integrated waveguide technology. *IEEE Transactions on Microwave Theory and Techniques*, 2015, vol. 63, no. 2, p. 422–432. DOI: 10.1109/TMTT.2014.2387272
- [6] HEBELKA, V., RAIDA Z. Koch slot loop antenna for wireless body-centric communication. *Microwave and Optical Letters*, 2014, vol. 56, p. 764–766. DOI: 10.1002/mop.28142
- [7] MORSHEDI, A., TORLAK, M. Measured comparison of dual-branch signaling over space and polarization diversity. *IEEE Transactions on Antennas and Propagation*, 2011, vol. 59, no. 5, p. 1678–1687. DOI: 10.1109/TAP.2011.2122210
- [8] ZHANG, Y., PANG, L., LIANG, X., et al. Propagation characteristics of circularly and linearly polarized electromagnetic waves in urban macrocell scenario. *IEEE Transactions on Vehicular Technology*, 2015, vol. 64, no. 1, p. 209–222. DOI: 10.1109/TVT.2014.2318839
- [9] LACIK, J., MIKULASEK, T. Substrate integrated waveguide rectangular ring slot antenna. In *Proceedings of the International Conference on Electromagnetics in Advanced Applications (ICEAA)*. Torino (Italy), 2011, p. 1164–1167. DOI: 10.1109/ICEAA.2011.6046515
- [10] KAZEMI, R., ALI SANDEGHZADEH, R., FATHY, A. A new compact wide band 8-way SIW power divider at X-band. In *Proceedings of the Loughborough Antennas and Propagation Conference (LAPC)*. Loughborough (United Kingdom), 2011, p. 1–4. DOI: 10.1109/LAPC.2011.6114098
- [11] GABRIEL, S., LAU, R. W., GABRIEL, C. The dielectric properties of biological tissues: III. Parametric models for the dielectric spectrum of tissues. *Physic in Medicine and Biology*, 1996, vol. 41, no. 11. P. 2271–2293.
- [12] LACIK, J., MIKULASEK, T., RAIDA, Z., URBANEC, T. Substrate integrated waveguide monopolar ring-slot antenna. *Microwave and Optical Technology Letters*, 2014, vol. 56, no. 8, p. 1865–1869. DOI: 10.1002/mop.28465

About the Authors ...

Petr VAŠINA was born in Brno. He received the M.Sc. from Brno University of Technology, Brno, Czech Republic, in 2013. He is currently a Ph.D. student at the Department of Radio Electronics, Faculty of Electrical Engineering and Communication, Brno University of Technology. He is a member of IEEE. His research interests include slot antennas and body-centric communication.

Jaroslav LÁČÍK received the M.Sc. and Ph.D. degrees from Brno University of Technology, Brno, Czech Republic, in 2002 and 2007, respectively. He is currently an Associate Professor at the Department of Radio Electronics, Faculty of Electrical Engineering and Communication, Brno University of Technology. His research interests are antennas, body-centric wireless communication, and computational electromagnetics. He is a member of IEEE.